POROSITY DEVELOPMENT DURING HEAT TREATMENT OF ALUMINUM-LITHIUM ALLOYS

J. Papazian, J. Wagner, W. Rooney

JOURNAL DE PHYSIQUE
Colloque C3, supplément au n°9, Tome 48, septembre 1987

POROSITY DEVELOPMENT DURING HEAT TREATMENT OF ALUMINUM-LITHIUM ALLOYS

J.M. PAPAZIAN, J.P.W. WAGNER and W.D. ROONEY

Corporate Research Center, Grumman Corporation, Bethpage, NY 11714-3580, U.S.A.

ABSTRACT

The development of a sub-surface layer of porosity during heat treatment has been studied in a variety of Al-Li alloys. Pure binary Al-Li alloys and three commercial materials were heat treated in air, vacuum and hydrogen for various lengths of time. Subsequent metallographic sectioning and polishing revealed the presence of a band of pores in the near-surface region extending approximately 300 μm into the sample after a 16 h heat treatment. This band of porosity is thought to arise from a Kirkendall effect due to the loss of lithium during heat treatment of the sample. The evolution of the spatial distribution of these pores was characterized with a quantitative image analyzer. The effects of prior surface preparation were also determined. The results showed that structural defects influenced pore nucleation and that environmental factors were also significant. A simultaneous pore healing process also occurred immediately adjacent to the external surface.

I. INTRODUCTION

Lithium is lost from the near surface region of aluminum-lithium alloys during elevated temperature heat treatment [1]. As a consequence of this loss, the near surface region becomes depleted in lithium and a lithium concentration gradient is established. This can cause several microstructural changes in the near-surface region, including, decreased hardness, a loss in tensile strength, increased electrical conductivity, and local recrystallization [2-10]. In addition, a narrow band of sub-surface porosity has been observed in the lithium depleted region of samples that have undergone extended elevated temperature heat treatments [1]. This band of porosity was assumed to be due to the condensation of vacancies that were part of the vacancy flux generated to compensate for the unequal diffusivities of lithium and aluminum. Because a sub-surface porous zone might have deleterious effects on surface sensitive properties of these alloys, an investigation into the characteristics of this porous zone was undertaken. The primary factors addressed were: alloy composition, heat treatment environment, sample surface preparation, sample microstructure and duration of heat treatment.

II. EXPERIMENTAL METHOD

Three commercially available Al-Li alloys were used. Plates of 8090 and 8091, 7.0 and 7.8 mm thick, respectively, were obtained from British Alcan Aluminium Co. in the T3 condition. The chemical analysis supplied with the 8090 showed in weight percent, 2.58% Li, 1.06% Cu, 0.56% Mg, 0.07% Fe, 0.02% Si, 0.021% Ti and 0.08% Zr. For 8091, the analysis showed 2.47% Li, 2.05% Cu, 0.58% Mg, 0.08% Si, 0.06% Fe, 0.02% Ti and 0.12% Zr. 2090 was obtained from Alcoa as a 12.5 mm thick plate in the T8E41 condition. Its composition was 2.7% Cu, 1.9% Li, 0.05% Fe, 0.03% Si, 0.003% Cr, <0.002% Mg and 0.16%Zr. Binary Al-Li alloys containing 1.0, 2.0, 3.1 and 4.0% Li, kindly supplied by A.P. Divecha of the Naval Surface Weapons Center, White Oak Laboratory, were also used. The casting and extrusion to a 6.25 by 37.5 mm cross section of these alloys has been previously described [3]. Sample coupons, 12.5 by 25 mm, were cut from the plate and extrusions such that the 25 mm dimension was aligned with the rolling or extrusion direction.

The surfaces of these coupons were prepared for heat treatment in a variety of ways that involved permutations of: as-received, sand-blasted, hand ground on SiC paper (5 or 18 μm grit size) electropolished (20 to 30 V in a 4:1 mixture of ethanol and perchloric acid between -30 and -20 °C for 10 to 15 minutes) and deformed by rolling to 15% RA.

Heat treatment was performed primarily in three different environments: vacuum, pure hydrogen and moist air. Several specimens were also heat treated in argon or dry air. The vacuum and hydrogen treatments were performed in a fused quartz tube sealed into an all metal, turbo pumped, high vacuum hydrogen charging system. Prior to the vacuum treatment, the sample chamber was baked out at 650 °C for several hours. During the treatment, the chamber pressure was 3 x 10^{-6} torr. Hydrogen treatments were performed in the same apparatus with a static hydrogen pressure of approximately 700 torr. The apparatus was evacuated and back filled three times prior to the heat treatment, and the hydrogen pressure remained constant to within 5 torr for the duration (16 h) of the heat treatment. Moist air treatments were performed in a vertical tube furnace. The high purity nitrogen:oxygen feed gas was bubbled through room temperature water before entering the furnace.

After heat treatment, the samples were cut in half transverse to the rolling direction, metallographically mounted and polished to 1 micron diamond finish on a Streuers automatic polishing machine. Metallographic observations were made using ordinary reflected light and also differential interference contrast, DIC. Quantitative analysis of the pore volume fraction was performed using a Leitz automated image analyzer.

III. RESULTS

A. Effects of Environment and Preparation

After heat treatment of 8091 for 16 h at 500°C in a vacuum, a band of fine pores was observed in the region between 75 and 250 μm from the original surface, Figure 1. At higher magnification, Figure 2, the pores appear to be empty and are approximately 0.5 to 3 μm in diameter. These pores will be referred to as Type I. When the same material was heat treated in moist air, the pores were denser, larger, and extended over a slightly broader band, Figure 3. At higher magnification some of these pores were up to 5 μm in diameter, and they often had an irregularly shaped particle at their base, Figure 4. The larger pores with particles will be termed Type II. Note that some Type I pores are also visible in Figure 4. When heat treated in hydrogen, fewer pores were observed, and those that were found were nearer to the external surface and appeared to be a mixture of both types described above. These observations were generally independent of the sample preparation and held true for surfaces that were as-received, sand-blasted, hand ground on 5 μm paper, electropolished or deformed to 15% RA. Likewise, 8090 behaved in a manner similar to 8091.

Limited observations were also made after heat treatment in dry air or argon. Results in dry air were very similar to those obtained in moist air. In argon, there was less porosity and it was confined to a band nearer the surface, approximately 50 to 200 μm deep, but pores were generally associated with particles, as in the samples treated in air.

B. Microstructural Effects.

It was generally observed that porosity was denser beneath a transverse, T, surface than a short transverse, S, surface, where T and S are the directions normal to the plane. This is illustrated in Figure 5 which shows the corner of a sample and portions of the T and S surfaces. The plane of this photomicrograph is L, as are all of the other micrographs. It can be seen that the band of porosity follows the contours of the surface and that there is a higher pore density near the T surface compared to the S surface. The pores sometimes were arranged in lines and occasionally outlined grain boundary triple points. Thus it appears that there is an enhanced probability of finding a pore on a grain boundary. With the pancake shaped grain structure existing in these samples, there is a higher number of grain boundaries intersecting the T face than the S. This appears to facilitate the formation of pores. Attempts to confirm the relationship between pores and grain boundaries by etching the sample failed due to the difficulty of identifying the pores after etching.

C. Effects of Alloy Composition

Two of the commercial alloys, 8090 and 8091, behaved in a similar manner for all of the permutations of surface condition and heat treat environment. The behavior of alloy 2090 was also similar to that of 8090 and 8091, but it was examined only after treatment in moist air with a hand ground or electropolished starting surface. The behavior of the binary Al-Li alloys was difficult to assess primarily because of the difficulty of obtaining a good metallographic polish. In general, there appeared to be some porosity present in the 2, 3, and 4% Li alloys while the 0 and 1% alloys had none. Large near surface blisters or bubbles were observed in the 3% binary Al-Li alloy with a hand ground surface after 16 h in moist air. One of these is shown in Figure 6. In addition to the blister, there are numerous smaller pores containing inclusions in the immediate vicinity of the blister. The blister may be caused by the evolution of hydrogen, and the presence of the small pores in the vicinity may indicate that hydrogen plays a role in their formation also.

D. Effect of Time

As the duration of the heat treatment increased, the pores became more dense and the distribution moved deeper into the sample. This is illustrated in the sequence of micrographs in Figure 7. These micrographs also show both Type I and Type II pores coexisting. The spatial distribution of the porosity in these samples was quantitatively characterized, and the results are shown in Figure 8a for 2090 with an electropolished starting surface and in Figure 8b for a hand ground starting surface. In these figures, the x axis represents distance from the external surface of the sample. Although there are obvious differences between the data in Figures 8a and 8b, these differences are not thought to be significant because of the generally variable spatial distribution of the pores. Equivalent quantitative results were also obtained for 8091 under the same conditions. These data illustrate the evolution of the porosity distribution profile. As the heat treatment time increased, more pores were formed, they occurred deeper into the sample, and the pores that were closest to the surface at short times tended to disappear. The development of a porosity denuded zone near the surface can be seen in the micrographs of Figure 7. The extent of this zone was measured and the results from this are plotted in Figure 9. The data roughly fit a $t^{1/2}$ law.

IV. DISCUSSION

These results show that the development of porosity is a relatively general phenomenon in Al-Li alloys. It occurred in all three of the commercial alloys and in the binary alloys. It occurred in various atmospheres including air, argon, hydrogen and vacuum, and it occurred after a wide variety of surface preparation techniques.

The porosity appears to be intimately related to lithium loss because the location and size of the porous zone corresponds exactly to the location and size of the lithium depleted region. If the porosity were solely due to the condensation of vacancies generated by the diffusion of lithium out of the sample, the amount of porosity expected can be easily calculated as follows.

The measured lithium concentration profile after 16 h is shown in Figure 10 [1]. Following Shewmon [11], the derivative of this curve combined with the lithium diffusivity gives the lithium flux as shown in Figure 11. The aluminum flux can be found in a similar manner and the difference between the two must be the vacancy flux, also plotted in Figure 11. Then, the rate of vacancy generation can be calculated as the derivative of the vacancy flux curve, and is shown in Figure 12. Since this is negative, it represents annihilation of vacancies. The shape and location of the calculated vacancy annihilation rate curve corresponds extremely well with the measured porosity distribution profiles (Figure 9). However, the curve in Figure 12 represents the instantaneous vacancy annihilation rate at 16 h. In order to calculate the total amount of porosity, it can be assumed that each vacancy annihilates and forms a pore at the location predicted by the annihilation rate curve. Thus, the instantaneous rate curves must be summed for the duration of the experiment. When this is done, the resultant curve looks like that in Figure 12 but flipped over to the positive y axis. The peak in the summation curve is shifted to the left and has a maximum of 0.05 volume fraction at approximately 75 μm from the external surface. This summation curve is shown as Figure 12 in reference 1 and its shape agrees less well with the measured distribution profiles. The calculated maximum volume fraction (0.05) is also higher than observed (0.01), but it is unlikely that every vacancy would annihilate at a pore. Many should annihilate at other defects. Despite this, the hypothesis that the pores are due to the condensation of vacancies generated because of the unequal fluxes of aluminum and lithium is very attractive. It is well supported by the observed evolution of the porosity distribution profile with time and is further supported by the observations that in the argon or hydrogen atmospheres, where less lithium is lost, fewer pores are observed and they are closer to the surface.

The observations of spherical, empty pores (type I) after heat treatment in a vacuum agrees well with the vacancy annihilation hypothesis. However, observations of a second type of pore (type II) containing inclusions or constituent particles after heat treatment in other environments, and of a higher pore density adjacent to presumed hydrogen blisters indicate that additional, environmental, factors may be important. The type II pores exhibit the same behavior (i.e. density, distribution, time dependence, etc.) as type I except for the presence of the inclusion. A possible explanation for this is that in environments where hydrogen may be present, pore nucleation is favored on existing particles in the microstructure. Alternatively, something may be transported into the alloy from the environment. This latter suggestion is considered unlikely.

The development and growth of a zone which is denuded of pores near the surface of the samples is not predicted by the analysis presented above. It is difficult to understand why pre-existing pores shrink and disappear as diffusion proceeds. It is possible that the nucleus of an explanation can be found by examining the over simplifications employed in the model described above. In particular, the alloys employed are not simple binaries, but contain significant amounts of copper (2090, 8090 and 8091) and magnesium (8090 and 8091). Magnesium is expected to be lost along with lithium [6], but the behavior of copper is not known. It is well accepted, however, that reducing the lithium content significantly increases the solubility of copper in Al-Li-Cu alloys [12]. At 500°C, reducing the lithium content from 2.7% to 1.3% increases copper solubility from practically zero to 4%. Thus, the presence of a lithium

concentration gradient will change the local chemical potential of copper and lead to development of a copper concentration gradient. This will be in a direction such that copper will tend to segregate near the lithium depleted external surface. This is the same location in which pores are observed to disappear as the heat treatment proceeds; thus, the arrival of copper in this region may cause the disappearance of the voids. Experiments are currently under way to measure the copper concentration gradient near the surface to check this hypothesis.

V. SUMMARY

A band of porosity has been observed in 2090, 8090 and 8091 in the lithium depleted near surface region after heat treatment at 500°C in vacuum, argon, hydrogen and wet or dry air.

The pores appear to be empty after a vacuum heat treatment, but are often associated with an inclusion particle after treatment in the other environments. Higher pore densities are observed near T surfaces than S, and near blisters.

The condition of the surface prior to heat treatment (i.e. as-received, ground, electropolished, deformed, etc.) is not a primary factor in the observation of porosity.

The location and evolution of the porosity distribution profile can be predicted by assuming that the pores are formed by the annihilation of vacancies required to compensate for the unequal fluxes of lithium and aluminum.

A porosity denuded zone appears near the surface and grows as heat treatment proceeds. It is suggested that the pores in this area are annihilated by a flux of copper atoms. The copper is thought to migrate into this region because the loss of lithium increases the local solubility of copper.

VI. ACKNOWLEDGMENTS

It is a pleasure to acknowledge discussions with P.N. Adler and R.L. Schulte, and the laboratory assistance of H. Baker. This work was performed as part of the Independent Research and Development program at Grumman Corp..

VII. REFERENCES

1. J.M. Papazian, R.L. Schulte and P.N. Adler, *Metall. Trans.*, 17A (1986) pp. 635-643.
2. J.A. Wert and A.B. Ward, *Scripta Met.*, 19 (1985) pp. 367-70.
3. M. Burke and J.M. Papazian in *Aluminum Lithium Alloys III*, ed. by C. Baker, P.J. Gregson, S.J. Harris and C.J. Peel, The Institute of Metals, London, 1986, pp. 287-293.
4. C.J. Peel, B. Evans and C.A. Baker in *Aluminum-Lithium Alloys III*, op. cit., pp.363-392.
5. H. Ueda, A. Matusi, M. Furukawa, Y. Miura and M. Nemoto, *J. Japan Inst. Metals*, 49 (1985) pp. 562-568.
6. S. Fox, H.M. Flower and D.S. McDarmaid, *Scripta Met.*, 20 (1986) pp. 71-74.
7. S. Fox, H.M. Flower and D.S. McDarmaid in *Aluminum-Lithium III*, op.cit., pp.263-272.
8. F. Abd El-Salam, A.I. Eatah and A. Tawfik, *Phys. Stat. Sol.*, (a) 75 (1983) pp. 379-384
9. J.M. Papazian, G.G. Bott and P. Shaw, *Proceedings 17th National SAMPE Technical Conference*, Kiamesha Lake, NY, Oct 22-24, 1985, pp. 688-699.
10. J.M. Papazian, G.G. Bott and P. Shaw, *Mater. Sci. and Engr.*, accepted for publication, 1987.
11. P.G. Shewmon: *Transformations in Metals*, 1st ed., McGraw-Hill, New York, NY, 1969, p. 57.
12. A.K. Hardy and J.W. Silcock, *J. Inst. Metals, London*, 84 (1955-56) pp. 423-28.

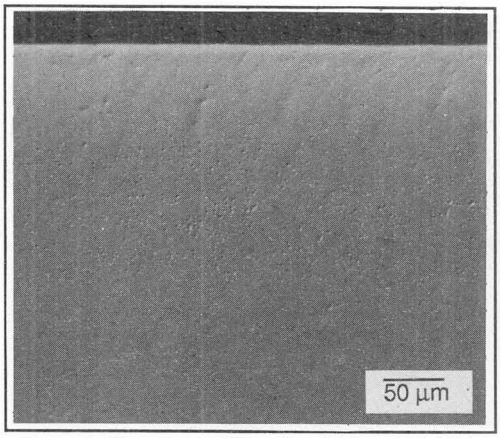

Figure 1. Porosity in 8091 after 16 h at 500 °C in a vacuum. DIC, 200X.

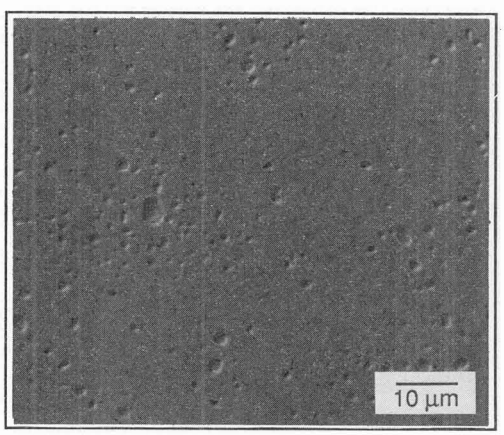

Figure 2. Enlarged view of the porous zone of the sample in Figure 1. DIC, 1000X.

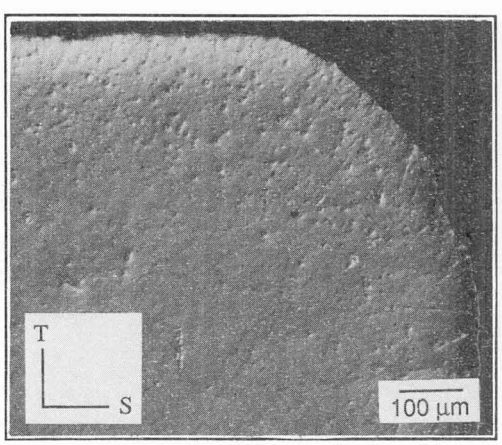

Figure 5. Corner of an 8091 sample after 16 h at 500°C in wet air. DIC, 100X.

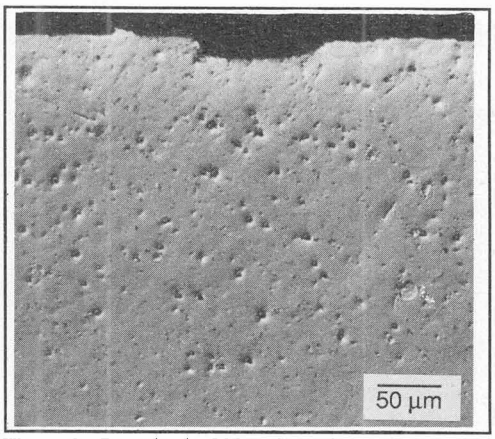

Figure 3. Porosity in 8091 after 16 h at 500 °C in wet air. DIC, 200X.

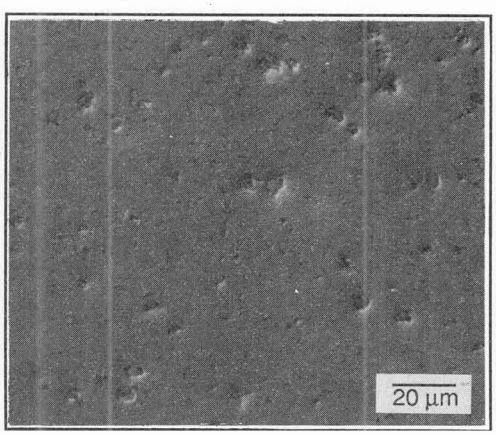

Figure 4. Enlarged view of the porous zone of the sample in Figure 3. DIC, 500X.

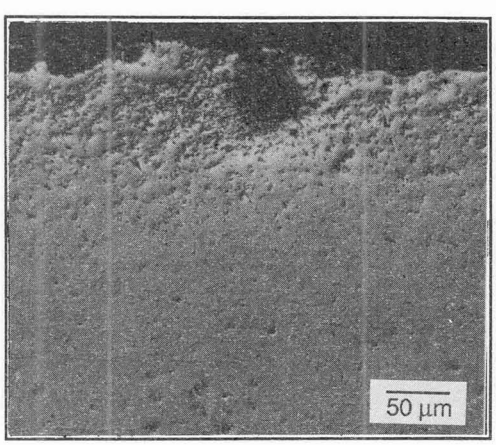

Figure 6. Near surface blister and associated porosity in Al-3.1% Li. 16 h at 500 °C, moist air.

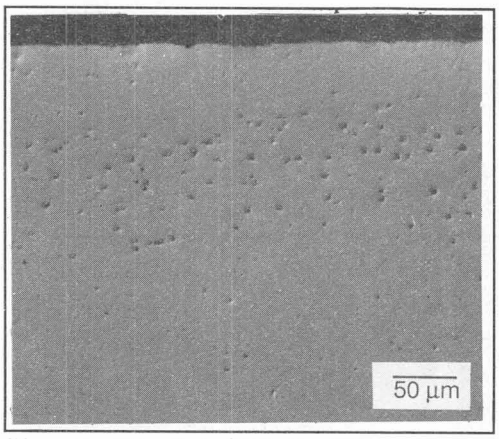

Figure 7a. Porosity in 8091 after 16 h at 500 °C in moist air. DIC, 200X.

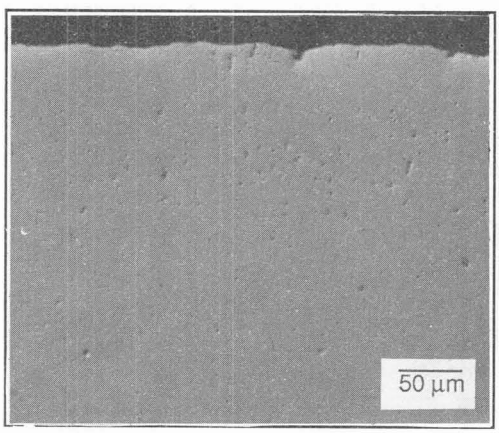

Figure 7b. After 8 h at 500°C.

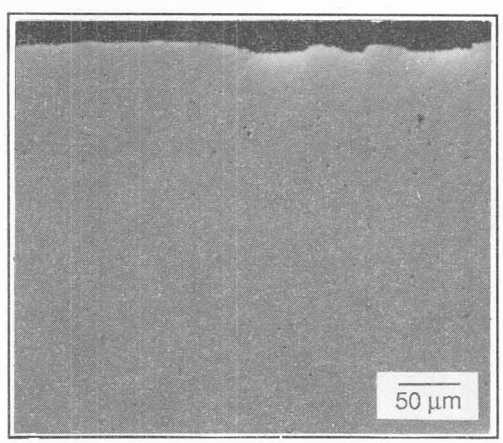

Figure 7c. After 4 h at 500°C.

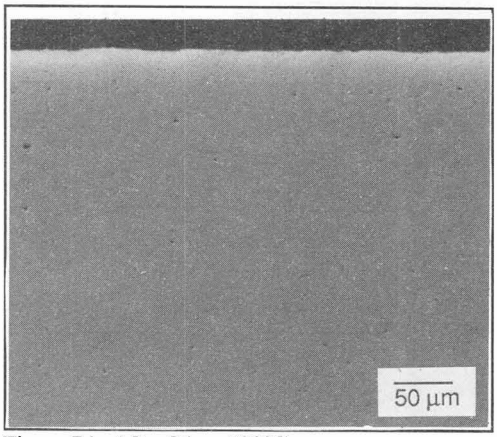

Figure 7d. After 2 h at 500°C.

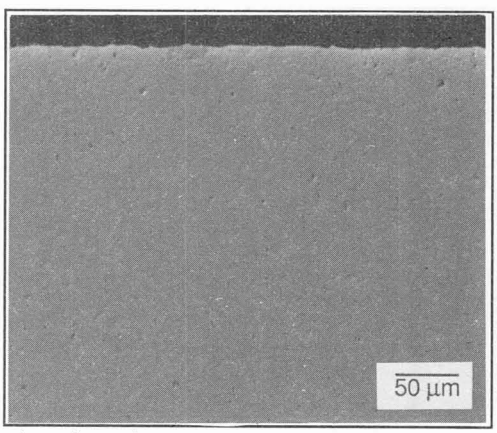

Figure 7e. After 1 h at 500°C.

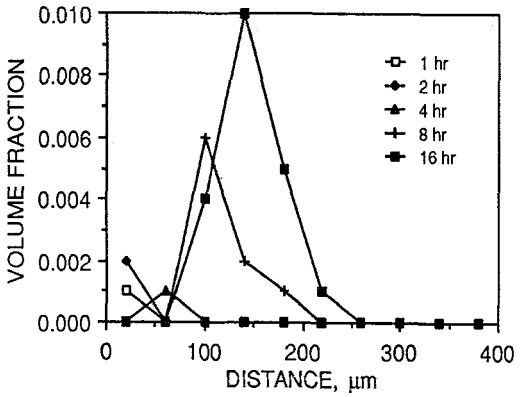

Figure 8a. The volume fraction of porosity in 2090 after heat treatment at 500°C in moist air. The starting surface was electropolished.

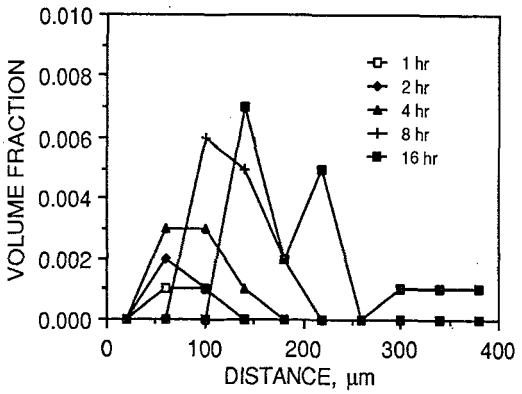

Figure 8b. The volume fraction of porisity in 2090 after heat treatment at 500°C in moist air. The starting surface was ground on 18 μm paper.

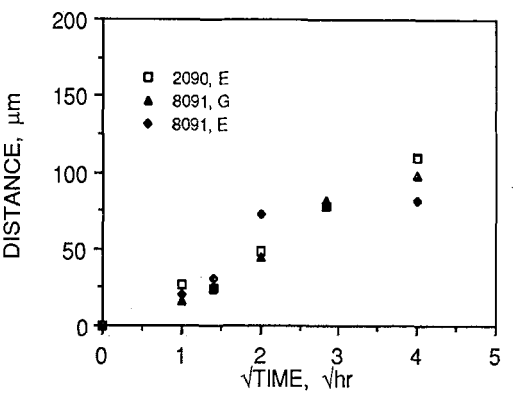

Figure 9. The depth of the porosity depleted zone as a function of time at 500°C in moist air. G represents hand ground on 18 μm paper and E represents electropolished starting surfaces.

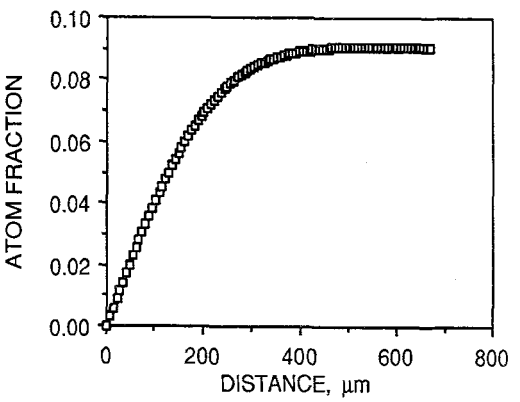

Figure 10. The lithium concentration profile after 16 h at 500°C (from reference 1).

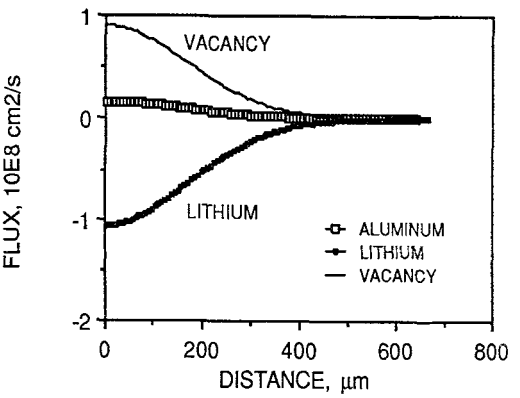

Figure 11. The flux of aluminum, lithium and vacancies after 16 h at 500°C.

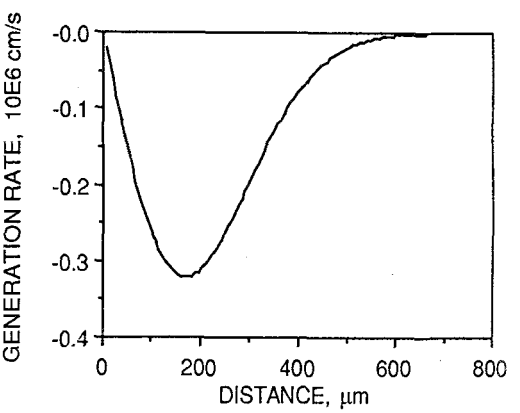

Figure 12. The rate of generation of vacancies atfter 16 h at 500°C. Since it is negative, this represents annihilation.